DOI: 10.1534/genetics.103.015198

Exploring the Evolution of Wolbachia Compatibility Types: A Simulation Approach

Sylvain Charlat,*[,1] Claire Calmet,[†] Olivier Andrieu* and Hervé Merçot*

**Institut Jacques Monod, Laboratoire Dynamique du Génome et Evolution, 75005 Paris, France and*
[†]*Museum National d'Histoire Naturelle, Service de Systématique Moléculaire, 75005 Paris, France*

Manuscript received March 14, 2003
Accepted for publication March 7, 2005

ABSTRACT

Wolbachia-induced cytoplasmic incompatibility (CI) is observed when males bearing the bacterium mate with uninfected females or with females bearing a different Wolbachia variant; in such crosses, paternal chromosomes are lost at the first embryonic mitosis, most often resulting in developmental arrest. The molecular basis of CI is currently unknown, but it is useful to distinguish conceptually the male and female sides of this phenomenon: in males, Wolbachia must do something, before it is shed from maturing sperm, that will disrupt paternal chromosomes functionality [this is usually termed "the modification (*mod*) function"]; in females, Wolbachia must somehow restore embryonic viability, through what is usually called "the rescue (*resc*) function." The occurrence of CI in crosses between males and females bearing different Wolbachia variants demonstrates that the *mod* and *resc* functions interact in a specific manner: different *mod resc* pairs make different compatibility types. We are interested in the evolutionary process allowing the diversification of compatibility types. In an earlier model, based on the main assumption that the *mod* and *resc* functions can mutate independently, we have shown that compatibility types can evolve through a two-step process, the first involving drift on *mod* variations and the second involving selection on *resc* variations. This previous study has highlighted the need for simulation-based models that would include the effects of nondeterministic evolutionary forces. This study is based on a simulation program fulfilling this condition, allowing us to follow the evolution of compatibility types under mutation, drift, and selection. Most importantly, simulations suggest that in the frame of our model, the evolution of compatibility types is likely to be a gradual process, with new compatibility types remaining partially compatible with ancestral ones.

MATERNALLY inherited elements are subject to sex-dependent selective pressures: their fitness is increased if females produce more females or better surviving females, regardless of possible detrimental effects to males (Cosmides and Tooby 1981; Frank and Hurst 1996). The endocellular bacterium Wolbachia illustrates nicely the possible outcomes of such selection, having evolved a variety of "sex manipulation strategies" that can be interpreted within this theoretical frame (reviewed in O'Neill *et al.* 1997; Stouthamer *et al.* 1999). Cytoplasmic incompatibility (CI) is one of them, probably the most common (reviewed in Hoffmann and Turelli 1997; Charlat *et al.* 2001a; Bourtzis *et al.* 2003). In embryos resulting from crosses between males that bear a CI Wolbachia and females that do not, paternal chromosomes are lost at the first mitosis (Callaini *et al.* 1996, 1997; Lassy and Karr 1996; Tram and Sullivan 2002), resulting in death in most cases (that is, in diploid species), but less often in male development (in some haplo-diploids). In contrast, if the female bears the bacterium, paternal chromosomes are not lost. Infected females thus produce on average more females than do uninfected ones, allowing infected cytoplasmic lines to invade uninfected populations. Infected males suffer a fertility deficit if uninfected females remain in the populations, since some proportion of their mating will be partially or fully sterile. But Wolbachia is not affected, as it is transmitted by females only.

The underlying mechanism remains to be elucidated. In males, Wolbachia must somehow affect the paternal nucleus before it is shed from maturing sperm, resulting in paternal chromosome loss after fertilization. In females, the bacterium must somehow prevent this loss and thereby rescue the embryo. This conceptual distinction between the male and female sides of CI was formalized by Werren (1997) through the modification/rescue (*mod/resc*) terminology.

Interestingly, crosses between infected males and infected females can also be incompatible, if the two partners bear different bacteria. The *mod* and *resc* functions thus seem to interact specifically: different Wolbachia

[1]*Corresponding author:* Biology Department, University College London, 4 Stephenson Way, London, NW1 2HE, United Kingdom. E-mail: s.charlat@ucl.ac.uk

can harbor different *mod resc* pairs, that is, different compatibility types. We are interested in the process that allows compatibility types to evolve. In an earlier study (Charlat *et al.* 2001b), we showed that compatibility types are not constrained by stabilizing selection, if *mod* and *resc* are determined by different genes, which, we think, is a reasonable assumption (Poinsot *et al.* 2003; see also Kose and Karr 1995; Callaini *et al.* 1997; Tram and Sullivan 2002). We suggested that compatibility types could change through a two-step process: the first involving drift on *mod* variations and the second involving selection on *resc* variations. This work highlighted the need for simulation-based models that would incorporate the effects of nondeterministic evolutionary forces. The present article is based on a simulation program developed in an attempt to fulfill this condition, allowing us to follow the evolution of compatibility types under mutation, drift, and selection.

THE MODEL

What defines a Wolbachia variant: Attempts have been made in earlier literature to translate the *mod resc* general formalization into more concrete models (reviewed in Poinsot *et al.* 2003): namely, the "slow-motion" model (Callaini *et al.* 1997; Tram and Sullivan 2002), the "titration-restitution" model (Kose and Karr 1995), and the "lock-and-key" model, more or less explicitly proposed in several articles (Breeuwer and Werren 1990; Hurst 1991; Werren 1997; Poinsot and Merçot 1999). In this later model *mod* and *resc* are seen as a lock and a key (that is, interacting physically and specifically with each other). In fertilized embryos, the lock, fixed on paternal material, would come into contact with the key, produced by Wolbachia in the egg. Depending on the conformation of the lock and the key, compatibility would range from 0 (total incompatibility) to 1 (total compatibility). In our opinion, this model is currently the most parsimonious and satisfactory (for a more detailed discussion of this issue see Poinsot *et al.* 2003). This view was implicitly the basis of our earlier theoretical work (Charlat *et al.* 2001b). The symbolism used here refers to the lock-and-key model more explicitly.

A Wolbachia variant is defined here by five parameters (summarized in Table 1). Two parameters define the compatibility type: the *lock* and the *key*. In practice, lock and key are modeled as sequences of S sites, with n possible states for each site (states 1, 2, . . . , n). In a cross between a male bearing Wolbachia i and a female bearing Wolbachia j, a compatibility score (C_{ij}) is calculated as the proportion of matching sites in the lock/key alignment. For example, with $S = 10$, we can have lock_i = 2222211111 and key_j = 2222222222, which gives the compatibility score $C_{ij} = 0.5$. Lock and key are comparable to the mod_C and $resc_C$ parameters in our earlier study (Charlat *et al.* 2001b), but with the notable difference that the current model allows partial compatibility if $S > 1$. MI (*mod* intensity) is the efficiency of the *mod* function; it corresponds to what is often referred to as "CI level," which can be measured in crosses between infected males and uninfected females. Biologically, MI can be seen as the proportion of infected males' sperm that is actually affected by CI. TE (transmission efficiency) is the proportion of infected eggs among those laid by infected females. Finally, FE (fitness effect) is the fecundity of infected females relative to that of uninfected females.

TABLE 1

Parameter definitions

Parameter	Definition
Lock	Identity of the *mod* function
Key	Identity of the *resc* function
S	Length of the lock and key sequences
n	No. of possible states at each site of the lock and key sequences
MI and MI_{max}[a]	Mod intensity: embryonic mortality in unidirectional CI
TE and TE_{max}[a]	Transmission efficiency
FE and FE_{max}[a]	Fitness effect: fecundity of infected females relative to uninfected
Mu	Mutation rate
N_e	Female host population size

[a] Upper limits can be set to values <1 for MI, TE, and FE. The upper limits for these parameters are denoted MI_{max}, TE_{max}, and FE_{max}, respectively.

The evolution of the TE and FE parameters is not in the focus of this study, as their evolutionary trajectories have been well described by the analytical approach (Turelli 1994): selection on Wolbachia always acts to increase infected females fecundity and maternal transmission efficiency. In other words, starting from any initial condition, these parameters will rapidly reach their maximum values under mutation and selection. However, FE and TE are still relevant to the model, as we can investigate the effect of setting upper limits <1 for these two parameters. For example, the model allows us to analyze the evolution of the lock and key parameters in populations where TE cannot exceed 0.9, that is, in populations where uninfected individuals can persist.

Similarly, the evolution of the MI parameter in panmictic populations has been previously worked out (Prout 1994; Turelli 1994): with random mating, MI is not under selection and evolves through drift only. However, keeping MI constant would impede the "realism" of our analysis. Consequently, the model includes the evolution of MI, although we do not focus on this aspect.

From one generation to the next: N_e males and N_e females actually reproduce at every generation; N_e is thus the effective population size of cytoplasmic genes. N_e females and N_e males are randomly chosen as parents on the basis of their frequencies at generation x. Sampling errors allow frequencies to drift. For every parental pair,

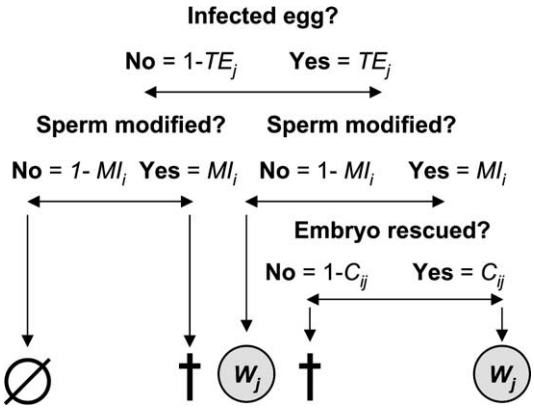

FIGURE 1.—How progeny is determined for any given cross. The male is infected by Wolbachia i, with parameters lock_i, key_i, MI_i, TE_i, and FE_i (but only MI_i and lock_i are relevant, since the other parameters are not expressed in males). The female is infected by Wolbachia j, with parameters lock_j, key_j, MI_j, TE_j, and FE_j (but only key_j, TE_j, and FE_j are relevant, since the other parameters are not expressed in females). If n_{egg} is the normal number of eggs laid per female, then E_{dead} (the number of dead embryos, single dagger), E_{uninf} (the number of living uninfected embryos, null set symbol), and E_{inf} (the number of living infected embryos bearing infection W_j, shaded circle) are the following:

$$E_{\text{dead}} = n_{\text{egg}} \times \text{FE}[\text{MI}_i(1 - \text{TE}_j) + \text{TE}_j \times \text{MI}_i(1 - C_{ij})]$$
$$E_{\text{uninf}} = n_{\text{egg}} \times \text{FE} \times (1 - \text{TE}_j) \times (1 - \text{MI}_i)$$
$$E_{\text{inf}} = n_{\text{egg}} \times \text{FE} \times \text{TE}_j[(1 - \text{MI}_i) + (\text{MI}_i \times C_{ij})].$$

progeny is determined as illustrated in Figure 1, allowing natural selection to act. The Wolbachia variants present at generation $x + 1$ are then submitted to mutation. Thus, generations x and $x + 1$ are separated by a round of drift, selection, and mutation. The five above-listed parameters are allowed to mutate independently from each other. Mutation rate per generation is denoted Mu. For the lock and key parameters, Mu is multiplied by S so that Mu gives the mutation rate per generation per site while Mu $\times$ S gives the mutation rate per generation per lock (or key) sequence. Mutations affecting the lock or the key sequences result in changing one of the S sites from its state to one of the $n - 1$ other states. Mutations affecting the MI, TE, or FE parameters result in adding $+0.05$ or -0.05 with equal probability to their initial value; if the initial value is maximum, then the mutation results in adding $+0.00$ or -0.05 with equal probability; conversely, if the initial value is minimum, then the mutation results in adding $+0.00$ or $+0.05$ with equal probability.

Assumptions: We are aware of the following assumptions in the model: (1) unbiased sex ratio; (2) nonoverlapping generations; (3) no population structure; (4) random mating; (5) no multiple infections [a given individual host is homogeneous with regard to Wolbachia infections; when a mutation gives rise to a new variant, its host is infected by this clone only (see DOBSON 2004 for an alternative model relaxing this assumption)]; (6) no recombination between Wolbachia variants; (7) no gene duplication (one bacterium bears only one *mod* and one *resc* function); and (8) no variations of host effects.

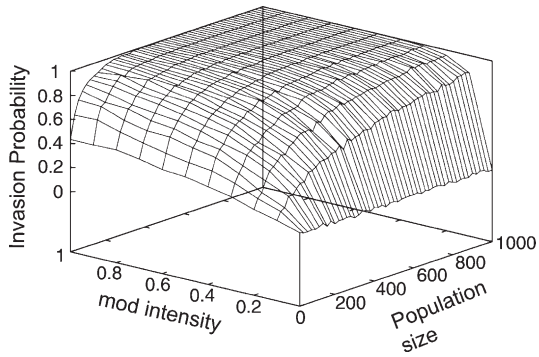

FIGURE 2.—Plot of invasion probability (estimated as the number of times over 1000 runs where Wolbachia finally got fixed) as a function of CI level (MI) and population size, for an initial frequency of 0.1. As expected, we observe that higher *mod* intensity allow Wolbachia to invade populations more efficiently. This is best seen in large populations, where drift has negligible effect as compared to selection.

VALIDATING THE MODEL

To validate the model, we tested whether it could retrieve earlier results, derived from the analytical approach. We first verified the basic prediction that CI allows Wolbachia to invade uninfected host populations, and more efficiently so if MI is high (Figure 2). We then investigated the combined effects of MI, TE, and FE on invasion dynamics. CASPARI and WATSON (1959), FINE (1978), and HOFFMANN *et al.* (1990) showed that if TE and/or FE are <1, Wolbachia does not invade unless it first reaches a threshold frequency depending on MI, TE, and FE. Above that point, infection frequency increases toward a stable infection frequency, which is not fixation if MI and TE are <1. As illustrated in Figure 3, the simulation and analytical approaches provide congruent predictions.

ILLUSTRATING RELEVANT PROCESSES WITHOUT RANDOM MUTATION

Before considering "realistic evolution," where an initial population can freely change under mutation, selection, and drift, we present here the results of simulations conducted without random mutation: several variants with specific properties are initially introduced and their frequencies followed over 1000 generations. These particular cases will allow the reader to understand which sequence of events can lead to which population state. With these processes in mind, the evolution of populations is analyzed more realistically in the next section.

Infection loss: Analytical models have revealed that elevated values of the MI, TE, and FE parameters facili-

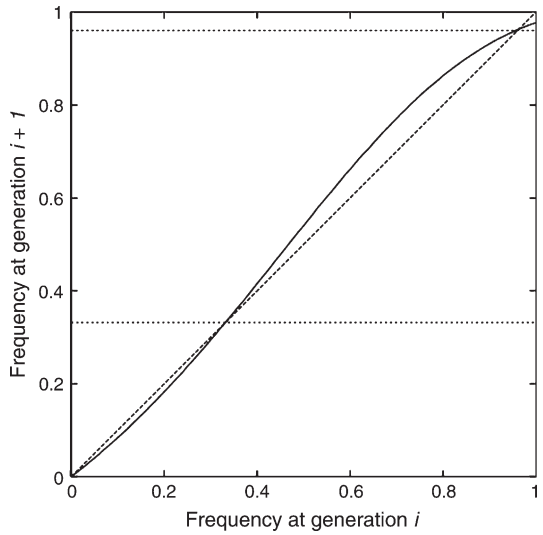

FIGURE 3.—The curve is a plot of infection frequency at generation $i + 1$ as a function of frequency at generation i, for a Wolbachia with the following properties: MI = 0.9, TE = 0.8, FE = 0.96. Any point below the $x = y$ line (dashed) indicates that infection frequency is decreasing; any point above indicates that it is increasing. Horizontal lines indicate the values predicted by the analytical approach for the lowest (unstable) and highest (stable) equilibriums (HOFFMANN *et al.* 1990). As expected, the curve crosses the $x = y$ line precisely forthese values. These results were obtained with a large population ($N_e = 10^6$), so that drift has negligible effects.

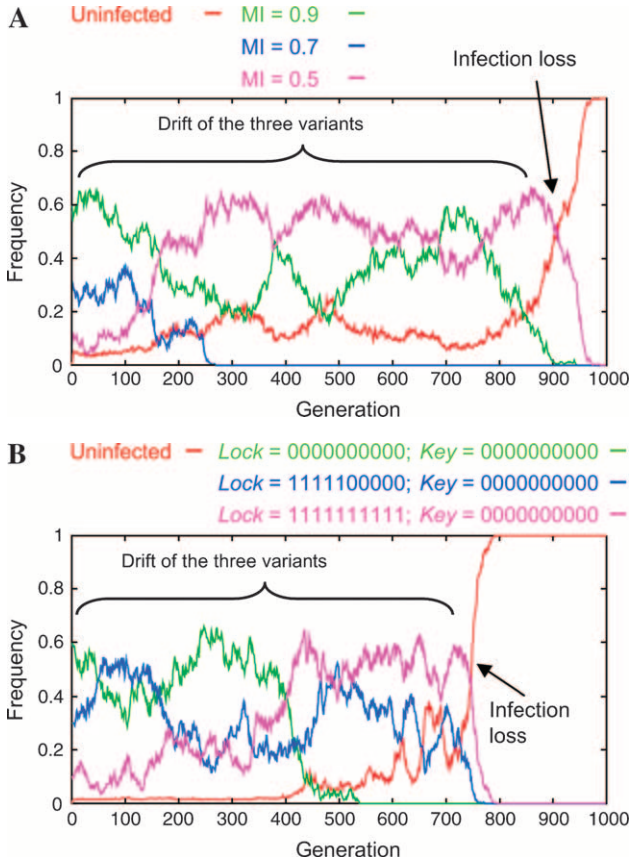

FIGURE 4.—The neutrality of MI and lock variations and their possible consequences on infection loss. Population size $N_e = 1000$. (A) The consequences of MI polymorphism. The three variants (MI = 0.9, 0.6, and 0.3) are initially introduced with respective frequencies 0.6, 0.3, and 0.1. The other parameters are not polymorphic: TE = 0.9, FE = 1, lock = 1111111111, key = 1111111111. Uninfected individuals rapidly reach the frequency expected on the basis of these parameters values. As expected from earlier analysis (PROUT 1994; TURELLI 1994), the frequencies of the three variants change through drift. These random changes affect the frequency of uninfected individuals, which increases as variants with low MI get more frequent through drift. After generation 900, the respective frequencies of the three variants are such that the unstable equilibrium value gets above the overall infection frequency, leading to the loss of Wolbachia. (B) The consequences of lock polymorphism. The three variants (lock = 1111111111, 2222211111, and 2222222222) are initially introduced with respective frequencies 0.6, 0.3, and 0.1. The other parameters are not polymorphic: MI = 0.9, TE = 0.9, FE = 1, key = 1111111111. Uninfected individuals rapidly reach the frequency expected on the basis of these parameters values. The frequencies of the three variants change through drift. These random changes affect the frequency of uninfected individuals, which increases as the two variants with a lock sequence different from 1111111111 get more frequent through drift. After generation 700, the respective frequencies of the three variants are such that the unstable equilibrium value gets above the overall infection frequency, leading to the loss of Wolbachia.

tate the stable maintenance of Wolbachia in host populations (HOFFMANN *et al.* 1990). They further showed that mutations decreasing TE or FE are always selected against (TURELLI 1994), so that the long-term evolution of these two parameters should stabilize the presence of Wolbachia. In contrast, mutations reducing MI are not selected against in panmictic populations (PROUT 1994; TURELLI 1994), so that MI is supposed to evolve under drift only (unless it is linked to other traits through pleiotropic effects). Increasing MI will stabilize the infection, but decreasing MI will have the opposite effect. Figure 4A illustrates how a random decrease of the average MI in the population can lead to infection loss: when Wolbachia variants with low MI get too frequent, the overall infection frequency (the stable equilibrium predicted by analytical models) decreases, while the threshold infection frequency (below which Wolbachia is lost deterministically) increases. Eventually, the population can get out of the conditions under which infection is maintained.

Less explicit in earlier analyses is the fact that variations affecting the lock parameter can also lead to infection loss. As detailed elsewhere (CHARLAT *et al.* 2001b), mutations affecting the lock sequence are not subject to selection, although they can give rise to self-incompatible, or "suicidal" Wolbachia. Figure 4B illustrates how this can lead to infection loss: as new lock variants (totally or partially self-incompatible) get too frequent by drift, the fitness gain provided by CI to infected females is lowered, which eventually leads to infection loss.

In summary, neutral variations of MI make CI less dele-

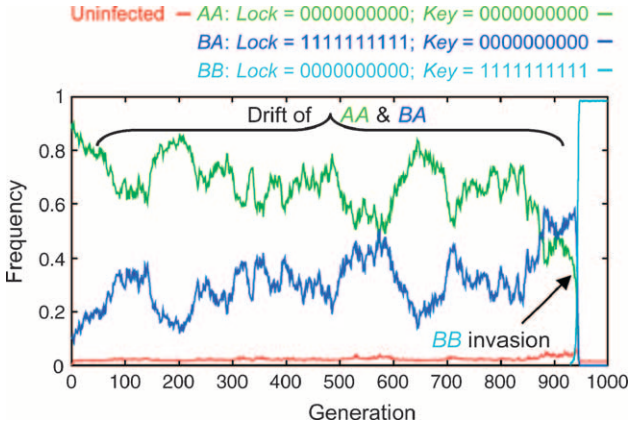

FIGURE 5.—The sequence of events leading to the invasion of new compatibility types. Population size N_e = 1000. Two variants (*AA*, $lock_A/key_A$; *BA*, $lock_B/key_A$; with $lock_A$ = 1111111111, $lock_B$ = 2222222222, key_A = 1111111111, and key_B = 2222222222) are initially introduced with respective frequencies 0.9 and 0.1. The other parameters are not polymorphic: MI = 0.9, TE = 0.9, FE = 1. As illustrated in B, this is a neutral polymorphism. A new variant (*BB*, $lock_B/key_B$) is introduced after generation 900, at a time where $f(BA) > f(AA)$. *BA* rapidly invades the population because $lock_B$ is more frequent than $lock_A$.

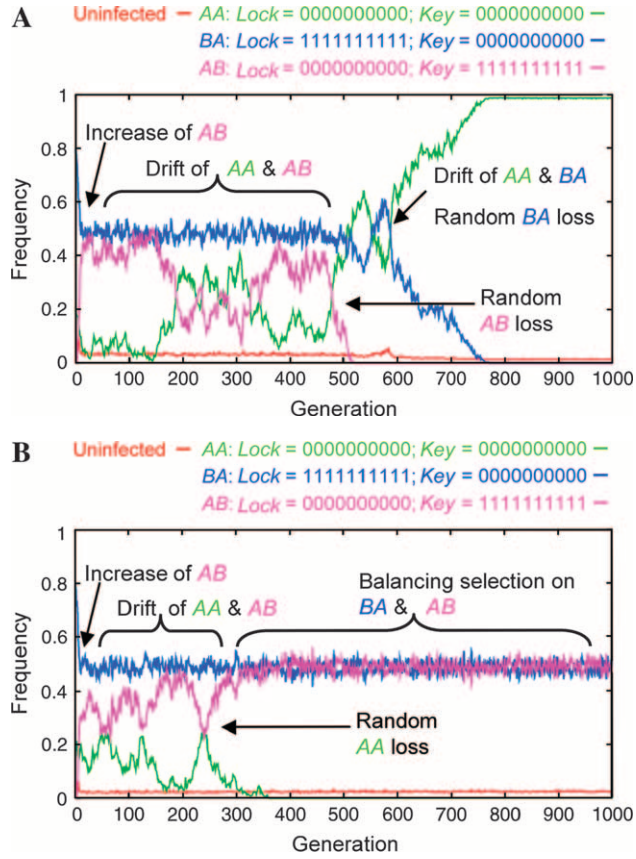

FIGURE 6.—How a "suicidal" polymorphism can be maintained by balancing selection. Population size N_e = 1000. Two variants (*AA*, $lock_A/key_A$; *BA*, $lock_B/key_A$; with $lock_A$ = 1111111111, $lock_B$ = 2222222222, key_A = 1111111111, key_B = 2222222222) are initially introduced with respective frequencies 0.2 and 0.8. The other parameters are not polymorphic: MI = 0.9, TE = 0.9, FE = 1. As illustrated in Figure 4B, this is a neutral polymorphism. A third variant (*AB*, $lock_A/key_B$) is introduced at the first generation, with frequency 0.001. In the very first generations, its frequency increases rapidly, because it bears key_B in a population where $lock_B$ is more frequent than $lock_A$. This increase stops when $f(lock_A) = f(lock_B)$, that is, when $f(BA) = f(AA) + f(AB)$. At that point $f(BA)$ is stably maintained, while $f(AA)$ and $f(AB)$ vary randomly and symmetrically, leading to the loss of *AB* (A) or *AA* (B). In A, the population goes back to the initial neutral polymorphism (with *AA* and *BA*), whereas in B, a stable polymorphism is reached, with $f(BA)$ and $f(AB)$ being maintained equal by balancing selection.

terious to uninfected females, while neutral variations of the lock make CI more deleterious to infected females. The final effect is the same in the two cases: net benefit to infected cytoplasmic lines is reduced.

Fixation of new compatibility types: As detailed elsewhere (CHARLAT *et al.* 2001b), random variations of lock can create the conditions for new compatibility types to invade populations. For the purpose of this section, let us define two different lock sequences, $lock_A$ (1111111111) and $lock_B$ (2222222222), and two different key sequences, key_A (1111111111) and key_B (2222222222). Consider a population harboring two Wolbachia variants: $lock_A/key_A$ (*AA*) and $lock_B/key_A$ (*BA*). This is a neutral polymorphism because the two variants harbor the same key sequence (key_A). The relative proportion of the two variants thus changes through drift only. A third variant [$lock_B/key_B$ (*BB*)] is introduced in the population. This new variant gets more frequent if the overall frequency of $lock_B$ exceeds that of $lock_A$, that is, if $f(BA) + f(BB) > f(AA)$. As $f(BB)$ increases, $lock_B$ becomes more frequent, so that the fitness of *BB* increases. Eventually, *BB* will get fixed, so that the compatibility type will have evolved from $lock_A/key_A$ to $lock_B/key_B$. Figure 5 shows how such a process can be visualized with our model.

Balanced suicidal polymorphism: Consider a population including two variants: $lock_A/key_A$ (*AA*) and $lock_B/key_A$ (*BA*). This is a neutral polymorphism: the relative proportion of *AA* and *BA* changes through drift only (CHARLAT *et al.* 2001b). Consider a new variant ($lock_A/key_B$ or *AB*) arising by mutation of the key in the *AA* variant. *AB* gets more frequent if the overall frequency of $lock_B$ exceeds that of $lock_A$, that is, if $f(BA) > f(AA) + f(AB)$. However, as *AB* becomes more frequent, $lock_B$ becomes less frequent, so that selection for *AB* is reduced. This leads to a situation where the three variants have the same fitness, when the frequency of $lock_A$ equals that of $lock_B$.

When such an equilibrium is reached, selection does not favor any Wolbachia variant in particular. However, simulation runs such as that presented in Figure 6 show that not all variants are maintained at stable frequencies. The frequency of *BA* appears to be stable, but $f(AA)$ and $f(AB)$ vary randomly and symmetrically, leading to the loss of either *AB* (Figure 6A) or *AA* (Figure 6B). If *AB* is lost, the population goes back to the initial neutral

polymorphism with *AA* and *BA*. In contrast, if *AA* is lost, the population reaches a stable polymorphism, with *BA* and *AB* at equal frequencies.

Notably, the initial conditions (the relative frequencies of *BA* and *AA* when *AB* is introduced) strongly affect the respective likelihoods of the outcomes described in Figure 6, A and B. The higher the initial $f(BA)/f(AA)$ ratio is, the higher is the frequency reached by the mutant *AB* under selection (in the very first generations following its introduction) and, in turn, the more likely is the outcome illustrated in Figure 6B, which depends directly on the $f(AA)/f(AB)$ ratio at the beginning of the "drift of *AA* and *AB*" stage (Figure 6, A and B, left).

A full understanding of the frequency variations during the drift of *AA* and *AB* stage is not straightforward (and not necessary for the following sections). The main point here is to show that a balanced suicidal polymorphism (illustrated in Figure 6B) can occur. The sequence of events leading to such balanced polymorphism involves a complex interaction between selection and drift: *AA* and *AB* are globally neutral relative to each other (although locally selection takes place) while the frequency of *BA* is locally and globally stabilized by selection. Figure 7 provides a more detailed explanation to the interested reader.

Neutral suicidal polymorphism and population extinction: Neutral variations of the lock function can greatly reduce host population mean fitness: as a $lock_B/key_A$ type gets frequent by drift, many crosses in the population are incompatible. Eventually, nothing opposes the fixation by drift of such a suicidal Wolbachia. If $MI < 1$, some proportion of the eggs can still survive. However, if $MI = 1$, and if $lock_B$ and key_A are totally incompatible, no viable progeny is produced, so that the host population simply goes extinct.

EVOLUTION UNDER MUTATION, DRIFT, AND SELECTION

Typology on population states: Having illustrated several possible sequences of events using specific combinations of lock/key pairs without random mutation, we now analyze how these different processes globally affect the evolution of populations, by allowing all parameters to mutate randomly. For the purpose of this analysis, let us define a typology on "population states," with six discrete states distinguished:

State 1: infection loss, when all individuals are uninfected.

State 2: population extinction, when no offspring is produced, due to the fixation by drift of a suicidal Wolbachia.

State 3: stability of compatibility types, when the initial lock/key pair is still predominant. Arbitrarily, we define "predominance" as a frequency >0.9, so that predominance of a type includes cryptic polymorphism, due to recurrent mutation.

State 4: predominance of a new compatibility type, when a new lock/key type, more compatible with itself than with the initial type, is at a frequency >0.9.

State 5: balanced suicidal polymorphism, when two types with higher cross-compatibility than self-compatibility (like $lock_B/key_A$ and $lock_A/key_B$), and only these two, are at frequencies >0.1.

State 6: this population state is peculiar in that it corresponds to all possible situations that are not described by the five other states. In practice, state 6 will describe mainly (i) populations harboring a neutral polymorphism (like $lock_A/key_A$ and $lock_B/key_A$) and (ii) populations where a suicidal type (like $lock_B/key_A$) is at a frequency >0.9. However, we do not rule out that state 6 might include others types of situations, potentially interesting but unidentifiable on the basis of our current understanding of the system.

This typology being defined, the evolution of populations can be depicted as transitions between population states over generations. Starting from an initial condition, different simulations can lead to very different patterns, because of random mutation and drift. To describe general tendencies, we can compile the results of a sufficient number of simulation runs, which will allow us to estimate the probability of the different population states over generations. In the following sections, we use this approach to explore the evolution of compatibility types under various conditions. Preliminary analyses (not shown) have been performed using high mutation rates over a short number of generations, to moderate calculation time. These have allowed us to identify four important factors: (1) the length of the lock and key sequences (parameter *S*); (2) the mutation rate (parameter Mu); (3) the population size (parameter N_e); and (4) the upper limits for TE, FE, and MI (parameters TE_{max}, FE_{max}, and MI_{max}) that will condition the possible maintenance of uninfected individuals in the populations. The effect of these factors is now examined in detail.

The effect of the lock/key structure: We defined lock and key as sequences of *S* sites. In a cross between a male bearing Wolbachia *i* and a female bearing Wolbachia *j*, the compatibility score (C_{ij}) is calculated as the proportion of matching sites in the lock/key alignment. To investigate the effect of varying *S* on the evolution of compatibility types, we followed 500 populations over 100,000 generations under two different conditions: $S = 1$ (Figure 8A) and $S = 10$ (Figure 8B). In these simulations, $N_e = 10^3$ and $Mu = 10^{-6}$ (see Figure 8 legend for details on other parameters).

When $S = 1$ (Figure 8A), we observe that the probability of the initial configuration (state 3: predominance of the initial type) decreases very slowly over generations.

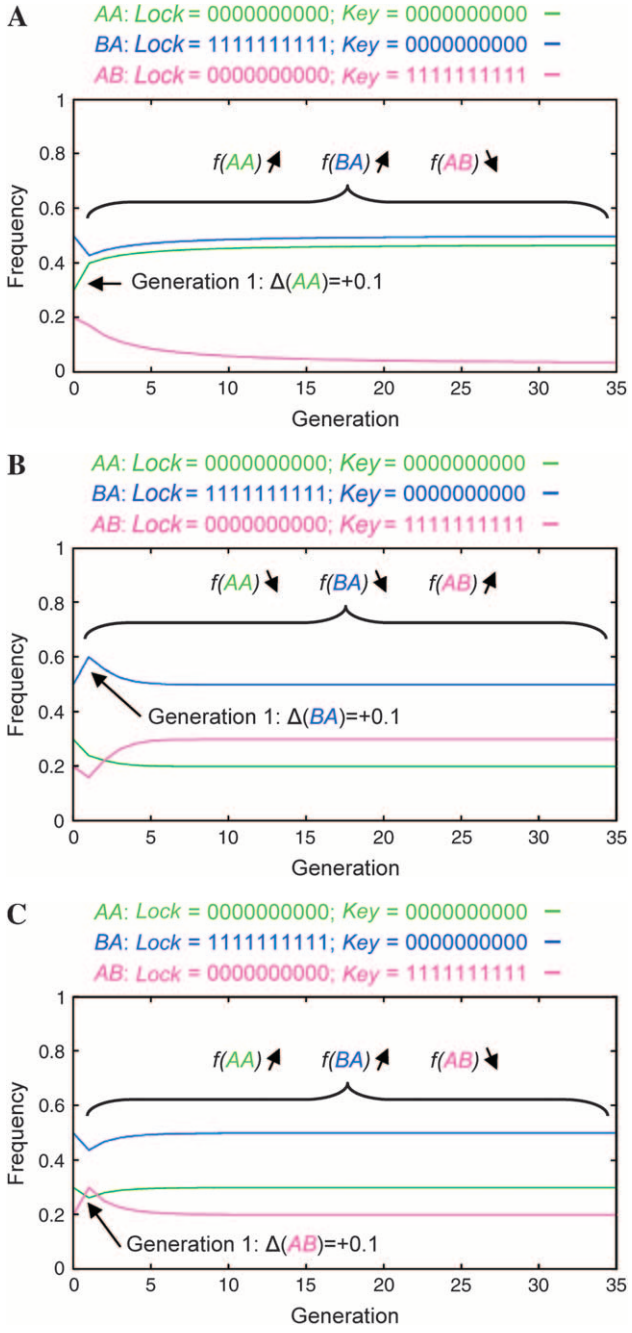

FIGURE 7.—How a population bearing *AA*, *BA*, and *AB* reacts to small random variations. The results were obtained with a simple deterministic model, that is, a model where selection takes place only after an initial and controlled "random" variation. This allows us to distinguish the effects of drift from those of selection. The fitness of the three variants is a function of their frequencies:

$$W_{AA} = f(AA) + f(AB)$$
$$W_{BA} = f(AA) + f(AB)$$
$$W_{AB} = f(BA).$$

The variants are initially introduced with respective frequencies $f(AA) = 0.3$, $f(BA) = 0.5$, $f(AB) = 0.2$. At that point, we have $W_{AA} = W_{BA} = W_{AB}$ but small random variations can occur. In A, B, and C, we consider the effect of an initial "random" increase ($\Delta = 0.1$) of $f(AA)$, $f(BA)$, and $f(AB)$, respectively. We assume that this random increase is accompanied by an evenly distributed decrease of the two other variants. In other words, if $f(AA)$ increases by $\Delta f(AA)$ then

$$\Delta f(BA) = -\Delta f(AA)\frac{f(BA)}{f(BA) + f(AB)}$$

and

$$\Delta f(AB) = -\Delta f(AA)\frac{f(AB)}{f(BA) + f(AB)}.$$

(A) A random increase of $f(AA)$ induces variations in the fitness of the three variants: W_{AA} and W_{BA} increase while W_{AB} decreases. Thus, following $\Delta f(AA)$, $f(AB)$ will decrease and $f(AA)$ and $f(BA)$ will increase deterministically, until a point where $f(BA) = f(AA) + f(AB)$, where selection ceases as all fitnesses are equal. The longer the time the population takes to get back equal to this point, the stronger the increase of $f(AA)$ relative to $f(AB)$ will be due to selection. A decrease of $f(AA)$ would have the exact symmetrical effect. (B) A random increase of $f(BA)$ induces variations in the fitness of the three variants: W_{AA} and W_{BA} decrease, while W_{AB} increases. Thus, following $\Delta f(BA)$, $f(AB)$ will increase, and $f(AA)$ and $f(BA)$ will decrease deterministically until a point where $f(BA) = f(AA) + f(AB)$, where selection ceases. The longer the time the population takes to get back equal to this point, the stronger the increase of $f(AB)$ relative to $f(AA)$ will be due to selection. A decrease of $f(BA)$ would have the exact symmetrical effect. (C) A random increase of $f(AB)$ induces variations in the fitness of the three variants: W_{AA} increases, W_{BA} increases, and W_{AB} decreases. Thus, following $\Delta f(AB)$, $f(AB)$ will decrease and $f(AA)$ and $f(BA)$ will increase deterministically, until a point where $f(BA) = f(AA) + f(AB)$, where selection ceases as all fitnesses are equal. This will always lead back to the initial situation, before the random increase of $f(AB)$. In summary, *AA* and *AB* are globally neutral relative to each other (although locally selection takes place) while the frequency of *BA* is locally and globally stabilized by selection.

Indeed, after 100,000 generations, predominance of the initial type is still observed in 90% of the simulations. Furthermore, we observe that among the remaining 10%, most populations have gone extinct due to fixation of a self-incompatible bacterium (state 2: population extinction). Thus, it appears that under these conditions, new compatibility types do not evolve. As illustrated in Figure 8B, things are clearly different when $S = 10$. Indeed, after 100,000 generations, <40% of the populations are still in the initial configuration, and the remaining 60% are in either state 4 (predominance of a new compatibility type) or state 6 (neutral polymorphism or predominance of partially suicidal Wolbachia). To apprehend the rationale behind these effects of *S* variations, one must distinguish two aspects of the differences observed between Figure 8A and 8B: (1) the slow *vs.* rapid decrease of state 3 (the initial configuration) and (2) the replacement of state 3 by state 2 (population extinction) *vs.* states 4 and 6. The explanation of difference 1 is the following: the mutation rate of the lock and key sequences is defined here as 10^{-6} per site; in other words, the overall mutation rate of the lock and key sequences is lower when the sequence is short (Fig-

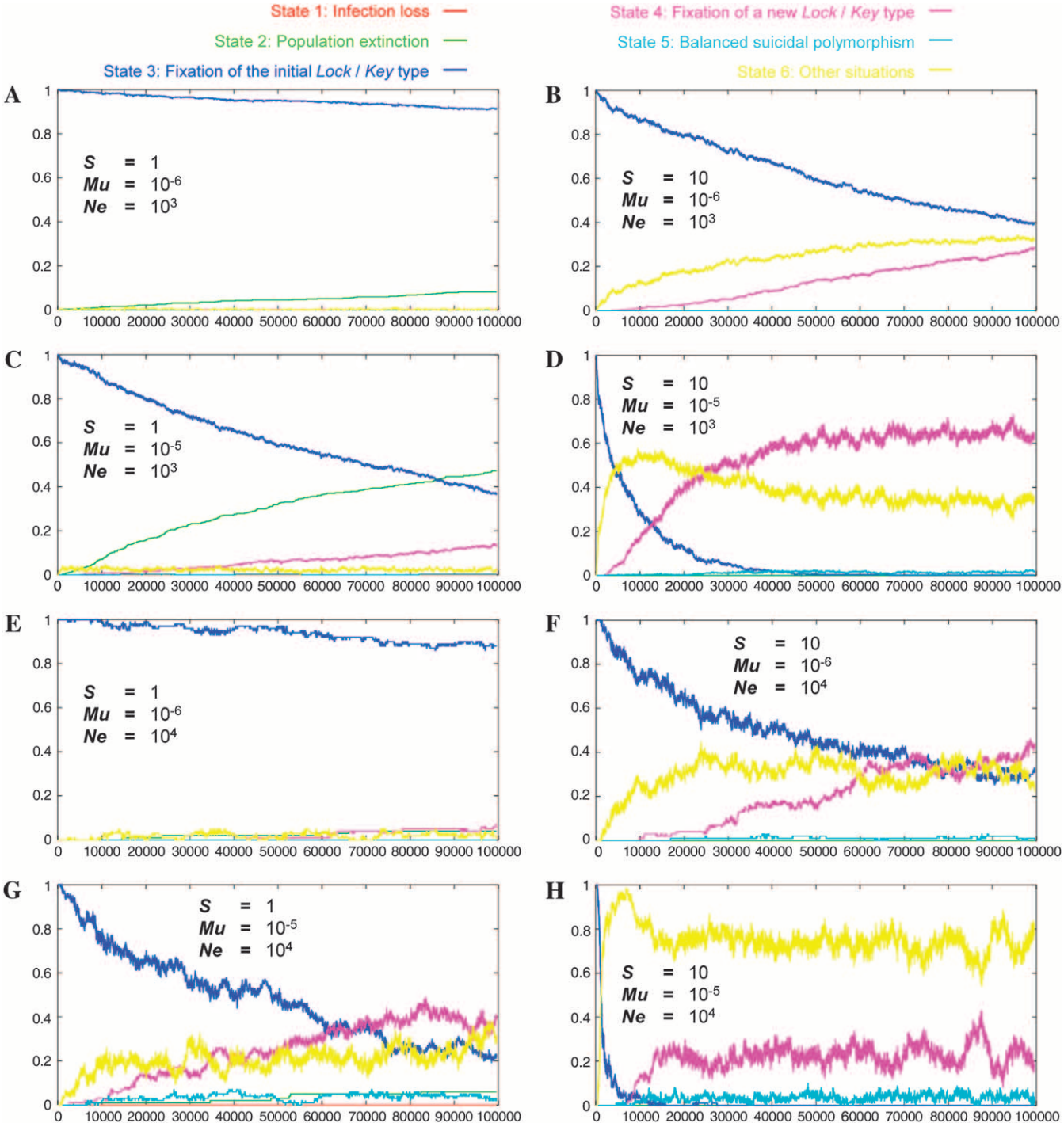

FIGURE 8.—The evolution of population states over 100,000 generations, for two different *S*-values ($S = 1$ and $S = 10$), two different Mu-values ($Mu = 10^{-6}$ and $Mu = 10^{-5}$), and two different N_e-values ($N_e = 10^3$ and $N_e = 10^4$). The curves plot the frequency of population states (*y*-axis) as a function of time (100,000 generations, *x*-axis), calculated over 500 simulation runs (A–D) or 100 simulation runs (E–H). Initial population: one single variant, totally self-compatible, with MI = 1, TE = 1, FE = 1, lock = 1111111111, key = 1111111111. The values of *S*, Mu, and N_e are given in A–H. Other parameters values are $n = 10$ and $MI_{max} = TE_{max} = FE_{max} = 1$. Note that for the lock and key parameters, Mu is multiplied by *S* so that Mu gives the mutation rate per site.

ure 8A) than when it is long (Figure 8B); the initial configuration is lost faster in Figure 8A because the overall mutation rates of the lock and key sequences are higher. The explanation of difference 2 (population extinction *vs.* other states) is less straightforward. In Figure 8A, where $S = 1$, compatibility between a given lock and a given key can be only 0 or 1. In other words, if the intensity of *mod* is maximum (that is, if MI = 1),

which is initially the case in these simulations, not a single viable egg is produced in incompatible crosses. Thus, if a suicidal type (with lock = 2 and key = 1) is fixed by drift, the host population goes extinct. In contrast, in Figure 8B, where $S = 10$, mutations of the lock and key sequences lead only to partial incompatibility. In other words, a suicidal type (partially suicidal) can reach fixation without leading the host population to extinction. In summary, the fact that populations go extinct in Figure 8A suggests that mutated lock sequences often reach fixation before a compatible key occurs by mutation. This readily leads the host population to extinction if $S = 1$, that is, if mutations of the lock sequence result in complete incompatibility.

We investigated in a similar way the effect of varying the n parameter (the number of possible states at each site in the lock and key sequences). The results are not presented graphically, as only minor quantitative effects were observed. Let us note that simply increasing the value of n tends to slow down the evolution of new compatibility types. This can be illustrated using the following example. Consider a population where a suicidal type (*e.g.*, with lock = 2 and key = 1) is frequent. If $n = 2$, mutations of the key sequence will give rise to the appropriate key (that is key = 2) with probability 1. In contrast, if $n = 10$, the appropriate mutation will occur with probability 1/9 only. In other words, increasing the value of n reduces the probability of favorable mutations to occur in the key sequence, resulting in slower evolution of compatibility types. In all simulations presented here, n is arbitrarily set at 10, a value that appeared to be a reasonable compromise between realism and computation time constraints.

The effect of mutation rates: The results discussed so far were obtained with $Mu = 10^{-6}$. To investigate the effects of mutation rates on the evolution of compatibility types, we repeated similar simulations to those presented in Figure 8, A and B (that is, with two different S values), under a 10 times higher mutation rate ($Mu = 10^{-5}$). The results are presented in Figure 8, C and D. By comparing Figure 8A and 8B with 8C and 8D, respectively, one can assess the effect of varying mutation rates for two different S values. In these simulations, $N_e = 10^3$ and $Mu = 10^{-5}$ (see Figure 8 legend for details on other parameters).

Three notable differences can be seen between Figure 8A and 8C: (1) in Figure 8C, <40% of populations are still in state 3 after 100,000 generations, as compared to 90% in Figure 8A; (2) in Figure 8C, >30% of the populations have gone extinct (state 2) after 100,000 generations, as compared to 10% in Figure 8A; and finally, (3) in Figure 8C, >20% of the populations harbor a new lock/key pair after 100,000 generations, as compared to 1% in Figure 8A. Difference 1 (that is, state 3 is less frequent in Figure 8C than in Figure 8A) illustrates that the initial lock/key type is lost faster when mutation rate is higher, as expected. It is notable that the rate of decrease of state 3 in Figure 8C is exactly the same as that observed in Figure 8B. This is consistent with the interpretation we gave when comparing Figure 8A with 8B: state 3 is lost faster when S is larger simply because the overall mutation rate of the lock and key sequences is increased. Difference 2 (that is, state 2 is more frequent in Figure 8C than in Figure 8A) suggests that extinction risk increases with mutation rate. This can be understood by remembering that extinction results from the fixation of a suicidal type (*e.g.*, with lock = 2 and key = 1). Mutations giving rise to such suicidal types being neutral, their rate of fixation depends only on the mutation rate (Kimura 1983). Difference 3 (that is, state 4 is more frequent in Figure 8C than in Figure 8A) suggests that the evolution of compatibility types is facilitated by increased mutation rates, which might seem straightforward. A subtle aspect deserves, however, to be discussed: in Figure 8C, the ratio state 4/state 2 (new type/extinction) is much higher than that in Figure 8A. To understand why, one must remember that spreading of new type (*e.g.*, with lock = 2 and key = 2) can occur only in populations where a suicidal type (*e.g.*, with lock = 2 and key = 1) is sufficiently frequent (see Figure 5). When the mutation rate is increased (as in Figure 8C), mutations giving rise to this new type are more likely to occur before the suicidal type has reached fixation (that is, before populations have gone extinct).

Consider now Figure 8, B and D. Three notable differences can be seen: (1) in Figure 8D, only a tiny remnant of populations are still in state 3 after 50,000 generations, as compared to 60% in Figure 8B; (2) in Figure 8D, the frequency of state 4 reaches a plateau of 60% after 50,000 generations, while no plateau was reached in Figure 8B after 100,000 generations; and finally, (3) in Figure 8D, a small but significant and stable proportion of populations is in state 5 (balanced suicidal polymorphism), while this state was not observed in Figure 8B. Difference 1 (that is, the complete loss of state 3 in Figure 8D) suggests that state 3 (predominance of the initial compatibility type) is unstable in the long term: mutation rate in Figure 8D is high enough for its inescapable loss to be observed after 50,000 generations only. Difference 2 (that is, state 4 reaches a plateau in Figure 8D) suggests that even with high mutation rates, the proportion of populations harboring a new compatibility type can never reach 1. Difference 3 (that is, state 5 is more frequent in Figure 8D) suggests that high mutation rates facilitate the occurrence of balanced suicidal polymorphism. Overall, it is interesting to note that the conditions used in Figure 8D ($Mu = 10^{-5}$ and $S = 10$) are such that 50,000 generations seem to be sufficient for the equilibrium distribution of population states to be observed. At equilibrium, populations are in state 4 (predominance of new type), state 5 (balanced suicidal polymorphism), or state 6 (neutral polymorphism or predominance of partially suicidal Wolbachia). This

equilibrium is clearly dynamic: populations themselves are not stable, but the probability of transitions between states 4, 5, and 6 is stable. It is likely that a similar equilibrium would be observed with a mutation rate of 10^{-6}, or even less, if populations were followed over a sufficiently large number of generations.

The effect of population size: The results discussed so far were obtained with $N_e = 10^3$. To investigate the effects of population size on the evolution of compatibility types, we repeated similar simulations to those presented in Figure 8, A–D (that is, four different combinations of *S* and Mu values), in smaller populations ($N_e = 10^2$) and larger populations ($N_e = 10^4$).

The results obtained with $N_e = 10^2$ are not presented graphically, as only minor quantitative effects were observed. Overall, reducing the population size from 10^3 to 10^2 has very little effect on the evolution of Wolbachia compatibility types. The conclusions drawn with $N_e = 10^3$ are retrieved: most importantly, the evolution of compatibility type occurs only when *S* is sufficiently large to prevent population extinction.

More interesting are the simulations performed with $N_e = 10^4$ (presented in Figure 8, E–H). Most importantly, we note that when $S = 1$, increasing population size reduces risks of population extinction. In Figure 8, E and G, state 2 (population extinction) is observed in only a small fraction of all simulations, contrasting with that observed in Figure 8, A and C. To understand this result, one must recall (i) that population extinction can occur when $S = 1$ due to neutral fixation of a mutated lock (*i.e.*, with lock = 2 and key = 1) and (ii) that the time separating the occurrence of a neutral allele and its fixation by drift is $4N_e$ on average (Kimura 1983). In other words, in large populations, the two mutation steps necessary for a new compatibility type to evolve often occur before extinction of the host population. This result is important with regard to the parameter space allowing the evolution of compatibility types: with large N_e, the evolution of compatibility types can occur even if $S = 1$. However, one should not conclude that large populations are protected from extinction in the long term: extinction being an absorbing state, it remains the ultimate fate of all populations if $S = 1$.

The effect of imperfect maternal transmission and fitness costs: The evolutionary forces acting on maternal transmission rates and fitness effects to the host have been thoroughly worked out by analytical models (Turelli 1994): increased transmission rates and decreased cost to the host are always selected for. In other words, whatever the initial situation in a population, TE and FE quickly reach their maximum possible value (TE_{max} and FE_{max}). In all simulations presented so far, we assumed that maternal transmission can be perfect and that infection is not necessarily costly to the host ($TE_{max} = 1$ and $FE_{max} = 1$), so that Wolbachia variants with $TE < 1$ or $FE < 1$ were observed only at very low frequency (mutation/selection balance). In this section, we assume that transmission efficiency cannot exceed 90% and that infection reduces the host fitness by at least 10% ($TE_{max} = FE_{max} = 0.9$). Similarly, we assume that the intensity of the *mod* function cannot exceed 90% ($MI_{max} = 0.9$). Such upper limits allow us to investigate the consequences of uninfected individuals persisting in the long term. With these upper limits for TE, FE and MI, we repeated simulations similar to those presented in Figure 8: we followed the evolution of populations under two *S* values ($S = 1$ or 10), two mutation rates ($Mu = 10^{-6}$ or 10^{-5}), and two different population sizes ($N_e = 10^3$ or 10^4). The results are presented in Figure 9.

To simplify the analysis, note first that the right columns of Figures 8 and 9 (where $S = 10$) are strikingly similar. In other words, setting upper limits for MI, TE, and FE does not affect the evolution of compatibility types when *S* is sufficiently large. We therefore focus on comparing the left columns of Figures 8 and 9 (where $S = 1$).

Let us consider Figure 9A ($Mu = 10^{-6}$, $S = 1$, $N_e = 10^3$, $MI_{max} = TE_{max} = FE_{max} = 0.9$) and compare it with Figure 8A (same values for Mu, *S*, and N_e, but $MI_{max} = TE_{max} = FE_{max} = 1$). In these two figures, the initial population state (state 3: predominance of the initial type) decreases at the same rate. In both cases, after 100,000 generations, predominance of the initial type is still observed in 90% of the simulations. In Figure 8A, state 3 is replaced only by state 2 (population extinction), contrasting with Figure 9A, where state 3 is replaced by state 1 (infection loss). The interpretation is the following: in Figure 8A, suicidal variants (*e.g.*, with lock = 2 and key = 1) can get fixed by drift, which causes population extinction; conversely, in Figure 9A (where $MI_{max} = TE_{max} = FE_{max} = 0.9$), the unstable equilibrium frequency (below which infection is deterministically lost) is increased by the presence of suicidal Wolbachia variants, so that the infection is always lost before the host population goes extinct. Thus, our model suggests that setting upper limits for MI, TE, and FE changes population extinction to infection loss. A similar conclusion is drawn from the comparison between Figures 8C and 9C (with $Mu = 10^{-5}$): in Figure 8C, state 3 is mainly replaced by state 2 (population extinction), while it is replaced by state 1 (infection loss) in Figure 9C.

Shifting to Figure 9, E and G (compared with Figure 8, E and G), we can assess the effect of MI_{max}, TE_{max}, and FE_{max} in large populations ($N_e = 10^4$). Most importantly, we note that risks of infection loss are only partially suppressed in large populations. In others words, even large populations are prone to infection loss when $S = 1$.

SUMMARY AND CONCLUDING REMARKS

We have used here a simulation approach to investigate the evolution of compatibility types under various conditions. Being aware that the flurry of conditions and results is difficult to keep track of, we summarize here our main findings, considering in turn the effect of each parameter (listed in Table 1).

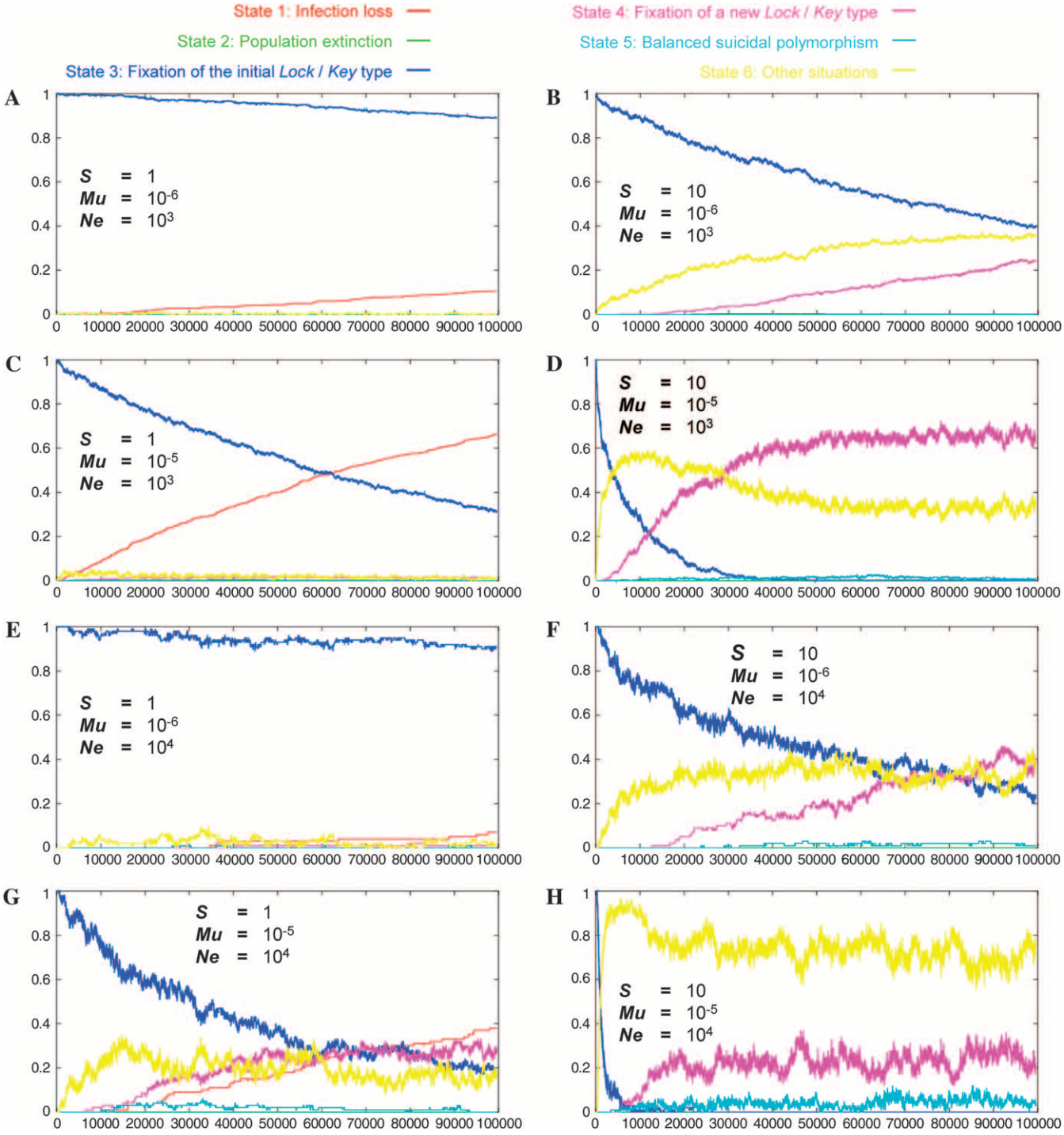

FIGURE 9.—See Figure 8 legend for details, except for the following: $MI_{max} = TE_{max} = FE_{max} = 0.9$.

n is the number of possible states at each site of the lock and key sequences; it conditions the potential diversity of compatibility types. We found that the value of n has only minor effects on the evolution of compatibility types. We note, however, that increasing the value of n tends to slow down the evolution of new compatibility types, as it reduces the probability of favorable mutations in the key sequence.

S is the length of the lock and key sequences; it conditions the potential for partial compatibility. If S is small (*i.e.*, $S = 1$), any mutation in the lock or key sequence leads to complete incompatibility. On the contrary, if S is large (*i.e.*, $S = 10$), mutation can give rise to different, but partially compatible lock and key. We found that the value of S has profound implications on the evolution of compatibility types: under small S values, population extinction or infection loss is likely to occur before new compatibility types get fixed. On the contrary, if S is large, populations are not prone to extinction or infection loss, allowing the evolution of compatibility types.

Mu is the mutation rate used in the model. We found that higher mutation rates accelerate the evolution of compatibility types, as expected. We also observed that high mutation rates increase risks of population extinction or infection loss when S is small.

N_e is the population size; it conditions the intensity of genetic drift and the mean time from mutation to fixation of neutral alleles. Most importantly, we observed that increasing population size tends to reduce risks of population extinction and, to a lesser extent, of infection loss. However, it must be kept in mind that population extinction and infection loss remain the only ultimate fates of all populations when S is small, since these are stable and absorbing states.

MI_{max}, TE_{max}, and FE_{max} are the upper limits of MI, TE, and FE, respectively; these condition the potential for uninfected individuals to persist in infected populations. We observed that setting these limits below their absolute maximum (that is, <1) prevents populations from going extinct when S is small. However, this does not facilitate the evolution of compatibility types, since risks of population extinction are replaced by risks of infection loss. Overall, we conclude that MI_{max}, TE_{max}, and FE_{max} do not affect the conditions under which the evolution of compatibility types is plausible.

In summary, our analysis points to S as the major parameter: the evolution of compatibility types most readily occurs when the lock and key sequences are sufficiently long, that is, when the lock/key pairs change gradually rather than suddenly. Interestingly, partial compatibility between distinct Wolbachia strains has been observed in Drosophila: the *w*Ri variant from *Drosophila simulans* is partially compatible with the *w*Mel variant from *D. melanogaster* (Poinsot *et al.* 1998). Similarly, the *w*Cer2 variant from *Rhagoletis cerasi* is partially compatible with *w*Mel and *w*Ri (Charlat *et al.* 2004; Riegler *et al.* 2004). Such empirical data support a model with $S > 1$.

In an alternative model, Dobson (2004) assumed that novel Wolbachia variants arising by mutation can coexist within a host individual together with the original infection. This analysis revealed interesting alternative routes for the evolution of compatibility types. In particular, it suggested that new types might evolve from an initial change in the *resc* function (mutation in the key sequence). One should note, however, that this remains plausible only if double infection is maintained over a sufficient number of generations. In other words, segregation from double to single infection (due to imperfect vertical transmission) has the potential to impede this particular process. Incorporating these aspects in the present model would allow one to assess the likelihood of this evolutionary trajectory.

In this article, we explored the evolution of compatibility under a wide variety of conditions. This analysis relies on heavy assumptions regarding the molecular mechanism of cytoplasmic incompatibility. Progress in this domain will accelerate now that the Wolbachia genome has been fully sequenced and analyzed (Wu *et al.* 2004). In turn, this should enrich the models and shed light on the evolutionary processes underlying the diversity of Wolbachia compatibility types.

We are deeply grateful to Thomas Pornin and Matthew Collette for their contribution to debugging. We also thank Frank Jiggins and two anonymous referees for critical reading and constructive comments.

LITERATURE CITED

Bourtzis, K., H. R. Braig and T. L. Karr, 2003 Cytoplasmic incompatibility, pp. 217–246 in *Insect Symbiosis*, edited by K. Bourtzis and T. Miller. CRC Press, Boca Raton, FL.

Breeuwer, J. A., and J. H. Werren, 1990 Microorganisms associated with chromosome destruction and reproductive isolation between two insect species. Nature **346:** 558–560.

Callaini, G., M. G. Riparbelli, R. Giordano and R. Dallai, 1996 Mitotic defects associated with cytoplasmic incompatibility in *Drosophila simulans*. J. Invertebr. Pathol. **67:** 55–64.

Callaini, G., R. Dallai and M. G. Riparbelli, 1997 *Wolbachia*-induced delay of paternal chromatin condensation does not prevent maternal chromosomes from entering anaphase in incompatible crosses of *Drosophila simulans*. J. Cell Sci. **110:** 271–280.

Caspari, E., and G. S. Watson, 1959 On the evolutionary importance of cytoplasmic sterility in mosquitoes. Evolution **13:** 568–570.

Charlat, S., K. Bourtzis and H. Merçot, 2001a *Wolbachia*-induced cytoplasmic incompatibility, pp. 621–644 in *Symbiosis: Mechanisms and Model Systems*, edited by J. Seckbach. Kluwer Academic, Dordrecht, The Netherlands.

Charlat, S., C. Calmet and H. Merçot, 2001b On the *mod resc* model and the evolution of Wolbachia compatibility types. Genetics **159:** 1415–1422.

Charlat, S., M. Riegler, I. Baures, D. Poinsot, C. Stauffer *et al.*, 2004 Incipient evolution of *Wolbachia* compatibility types. Evolution **58:** 1901–1908.

Cosmides, L. M., and J. Tooby, 1981 Cytoplasmic inheritance and intragenomic conflict. J. Theor. Biol. **89:** 83–129.

Dobson, S. L., 2004 Evolution of Wolbachia cytoplasmic incompatibility types. Evolution **58:** 2156–2166.

Fine, P. E. M., 1978 On the dynamics of symbiont-dependent cytoplasmic incompatibility in Culicine mosquitoes. J. Invertebr. Pathol. **30:** 10–18.

Frank, S. A., and L. D. Hurst, 1996 Mitochondria and male disease. Nature **383:** 224.

Hoffmann, A. A., and M. Turelli, 1997 Cytoplasmic incompatibility in insects, pp. 42–80 in *Influential Passengers: Inherited Microorganisms and Arthropod Reproduction*, edited by S. L. O'Neill, A. A. Hoffmann and J. H. Werren. Oxford University Press, Oxford.

Hoffmann, A. A., M. Turelli and L. G. Harshman, 1990 Factors affecting the distribution of cytoplasmic incompatibility in *Drosophila simulans*. Genetics **126:** 933–948.

Hurst, L. D., 1991 The evolution of cytoplasmic incompatibility or when spite can be successful. J. Theor. Biol. **148:** 269–277.

Kimura, M., 1983 *The Neutral Theory of Molecular Evolution*. Cambridge University Press, Cambridge, UK.

Kose, H., and T. L. Karr, 1995 Organization of *Wolbachia pipientis* in the *Drosophila* fertilized egg and embryo revealed by an anti-*Wolbachia* monoclonal antibody. Mech. Dev. **51:** 275–288.

Lassy, C. W., and T. L. Karr, 1996 Cytological analysis of fertilization and early embryonic development in incompatible crosses of *Drosophila simulans*. Mech. Dev. **57:** 47–58.

O'Neill, S. L., A. A. Hoffmann and J. H. Werren, 1997 *Influential Passengers: Inherited Microorganisms and Arthropod Reproduction*. Oxford University Press, Oxford.

Poinsot, D., and H. Merçot, 1999 *Wolbachia* can rescue from cytoplasmic incompatibility while being unable to induce it, pp. 221–234 in *From Symbiosis to Eukaryotism—Endocytobiology VII*, edited by E. e. a. Wagner. Universities of Geneva and Freiburg, Breisgau, Germany.

Poinsot, D., K. Bourtzis, G. Markakis, C. Savakis and H. Merçot, 1998 Wolbachia transfer from *Drosophila melanogaster* into *D. simu-*

lans: host effect and cytoplasmic incompatibility relationships. Genetics **150:** 227–237.

Poinsot, D., S. Charlat and H. Merçot, 2003 On the mechanism of Wolbachia-induced cytoplasmic incompatibility: confronting the models with the facts. BioEssays **25:** 259–265.

Prout, T., 1994 Some evolutionary possibilities for a microbe that causes incompatibility in its host. Evolution **48:** 909–911.

Riegler, M., S. Charlat, C. Stauffer and H. Merçot, 2004 *Wolbachia* transfer from *Rhagoletis cerasi* to *Drosophila simulans*: investigating the outcomes of host-symbiont coevolution. Appl. Environ. Microbiol. **70:** 273–279.

Stouthamer, R., J. A. Breeuwer and G. D. Hurst, 1999 *Wolbachia pipientis*: microbial manipulator of arthropod reproduction. Annu. Rev. Microbiol. **53:** 71–102.

Tram, U., and W. Sullivan, 2002 Role of delayed nuclear envelope breakdown and mitosis in *Wolbachia*-induced cytoplasmic incompatibility. Science **296:** 1124–1126.

Turelli, M., 1994 Evolution of incompatibility-inducing microbes and their hosts. Evolution **48:** 1500–1513.

Werren, J. H., 1997 Biology of *Wolbachia*. Annu. Rev. Entomol. **42:** 587–609.

Wu, M., L. V. Sun, J. Vamathevan, M. Riegler, R. Deboy *et al.*, 2004 Phylogenomics of the reproductive parasite Wolbachia pipientis wMel: a streamlined genome overrun by mobile genetic elements. PLoS Biol. **2:** E69.

Communicating editor: H. G. Spencer